Direct Electrochemistry of Horseradish Peroxidase Embedded in Nano-Fe_3O_4 Matrix on Paraffin Impregnated Graphite Electrode and Its Electrochemical Catalysis for H_2O_2†

GONG, Jing-Ming(龚静鸣) LIN, Xiang-Qin*(林祥钦)
Department of Chemistry, University of Science and Technology of China, Hefei, Anhui 230026, China

Fe_3O_4 particles coated with acrylic copolymer (ACP) of about 5—8 nm in diameter were synthesized and used for immobilization of horseradish peroxidase (HRP). Direct electrochemistry of HRP embedded in the nanosized Fe_3O_4 solid matrix modified paraffin impregnated graphite electrode (PIGE) was achieved, which is related to the heme Fe(III)/Fe(II) conversion of HRP. Cyclic voltammetry gave a pair of reproducible and well-defined redox peaks at about E_m of −0.295 V vs. SCE. The standard rate constant k_s was determined as 2.7 s^{-1}. It demonstrated that the nano-Fe_3O_4 solid matrix offers a friendly platform to assemble the HRP protein molecules and enhance the electron transfer rate between the HRP and the electrode. UV-Vis absorption spectra and FTIR spectra studies revealed that the embedded HRP retained its native-like structure. The HRP/Fe_3O_4/PIGE showed a strong catalytic activity toward H_2O_2. The voltammetric response was a linear function of H_2O_2 concentration in the range of 10—140 μmol/L with detection limit of 7.3 μmol/L (s/n = 3). The apparent Michaelis-Menten constant is calculated to be 0.42 mmol/L.

Keywords horseradish peroxidase (HRP), nano-Fe_3O_4, direct electrochemistry, electrochemical catalysis, hydrogen peroxide

Introduction

Horseradish peroxidase (HRP, FW approx. 44000) is a well-known heme-containing redox enzyme, which is widely used for catalytic oxidation of a wide variety of substrates.[1,2] Direct electron transfer (dET) between the embedded enzyme and electrodes can drive enzyme-catalyzed reaction and serve as a basis of biosensors, biomedical devices. The dET has become an important research area, and aroused many interest.[3,4] However, dET between the electrode surface and the electroactive prosthetic groups of redox enzyme is prohibited owing to the deep buried nature of the active site, adsorption denaturation of macromolecules onto electrodes, and slow mass transfer rate of proteins toward electrodes. Therefore, immobilization of enzyme onto electrode surface for direct electrochemistry has become a more and more important area of research.[5-11] Many efforts have been made to facilitate the electron transfer, including immobilization of proteins in polymeric film,[8,11] lipid film,[12,13] and nanocrystalline TiO_2 film.[14] Biocompatible ferromagnetic material has gained intense research in biomedical and biotechnological applications.[15-17] Nanosized magnetite is widely used in this field as a new kind of functional nano-material. It has been reported that the ferromagnetic particles can favorably interact with enzyme by active groups such as —OH, —COOH, —NH_2, without denaturation.[18,19] However, the application of nano-magnetic material Fe_3O_4 as a solid matrix to immobilize HRP for facilitating the dET has not been reported in the literature. In this paper, an investigation of the interaction between HRP and nano-Fe_3O_4 matrix, dET of HRP embedded on the nano-Fe_3O_4 at a paraffin impregnated graphite electrode (PIGE) and its catalytic activity toward hydrogen peroxide are described.

Experimental

Chemicals and reagents

Peroxidase (EC 1.11.1.7, from horseradish, 250 U/mg, pI = 7.2) was purchased from the Sino-American Biotechnology. Bovine serum albumin (BSA) was obtained from the Shanghai Blood Research Institute of the Chinese Academy of Agriculture Sciences. Glutaraldehyde (25% V/V solution in water) was from Acros, USA. Acrylic acid/acrylate copolymer (ACP) (FM, 4500) was from Rohm & Hass, USA. Hydrogen peroxide (30% V/V solution) was from the Chemical Reagents Company of Shanghai (China). All other chemicals were of analytical grade. A 10 mmol/L phosphate buffer solution (pH = 6.1) containing 50 mmol/L KCl (KCl-PBS) was used as supporting electrolyte. By mixing of stock solutions of KH_2PO4, K_2HPO_4, H_3PO_4 and K_3PO_4, 10 mmol/L PBS with various pH values were prepared. Double dis-

* E-mail: xqlin@ustc.edu.cn; Tel.: 86-551-3606646; Fax: 86-551-3601592
Received January 22, 2003; revised and accepted May 5, 2003.
Project supported by the University of Science and Technology of China (Nos. ky1212 and ky2216).
†Dedicated to Professor ZHOU Wei-Shan on the occasion of his 80th birthday.

tilled water was used. High purity nitrogen was used for removing oxygen.

Apparatus

A computer-based electrochemical workstation (CHI 660A, Shanghai, China) was used for voltammetric measurements. A three-electrode system was used, which was composed of a saturated calomel electrode (SCE), a platinum wire counter electrode, and a working electrode. The electrochemical solution was bubbled with nitrogen for 15 min to remove oxygen prior to measurement and the solution was kept under nitrogen atmosphere during experiment. All experiments were carried out at room temperature (15 ± 1) ℃.

X-Ray diffraction (XRD) was performed with a D/Max-γ A powder diffractometer (Rigaku) using a Cu Kα source ($\lambda = 0.154178$ nm) at 30 kV, 20 mA. Transmission electron micrograph (TEM) was recorded by an H800 transmission electron microscope (Hitachi; Tokyo, Japan). UV measurements were performed with a Tu-1901 (Beijing, China) UV-vis spectrophotometer. FTIR spectra were obtained by using a Model VECTOR-22 FTIR spectrometer (Bruker, Switzerland).

Preparations of nano-Fe_3O_4

The nano-Fe_3O_4 particles coated with ACP were prepared via the chemical co-precipitation according to the reported method.[20] $FeCl_3 \cdot 6H_2O$ (1.1 g, 4 mmol) and 0.4 g of $FeCl_2 \cdot 4H_2O$ (2 mmol) were dissolved in 100 mL of deoxygenated water. A 25% $NH_3 \cdot H_2O$ solution in minor excess was added to the solution under mechanical stirring until the pH reached to 10 at 50 ℃. Thereafter, the reaction was carried out in a bath at 60 ℃. ACP, as a dispersant, was immediately added and its concentration was controlled up to 1.5 g/L. The crystal growth was allowed to proceed at 80 ℃ for 30 min. A dark precipitate was finally isolated from the suspension by magnetic decantation. After washing with deoxygenated water and anhydrous alcohol three times respectively, the purified product was obtained. It was re-dispersed in anhydrous alcohol solution for XRD and TEM characterization.

Fig. 1 shows the XRD spectrum of the prepared Fe_3O_4 particles. In the 2θ range of 20°—70°, the peak positions at corresponding 2θ value are indexed as (2 2 0), (3 1 1), (2 2 2), (4 0 0), (4 2 2), (5 1 1) and (4 4 0), respectively. From these diffraction data, it could be inferred that spinel structure Fe_3O_4 has been synthesized.[20,21] The result of TEM (Fig. 2) displayed that the Fe_3O_4 particles were nanosized with sphere shape of average size of about 5—8 nm.

Fabrication of HRP *electrode*

The basic graphite disk electrode was made by pressing a piece of spectral graphite rod into a Teflon tube of 6 mm i.d and 10 mm o.d. and led out using a copper wire and silver adhesives. Then the graphite disk electrode was saturated with paraffin under infrared light for 30 min. After polishing the electrode surface successively with metallorgraphic SiC paper of different grades, the PIGE was sonicated in anhydrous alcohol and double distilled water for 5 min respectively. Then the PIGE was rinsed with water thoroughly, dried under nitrogen atmosphere and ready for use.

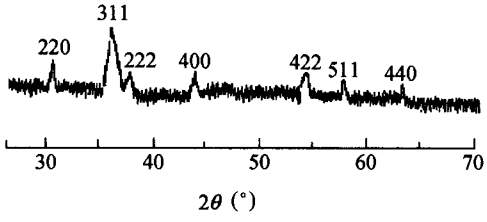

Fig. 1 XRD spctrum of synthesized Fe_3O_4 particles.

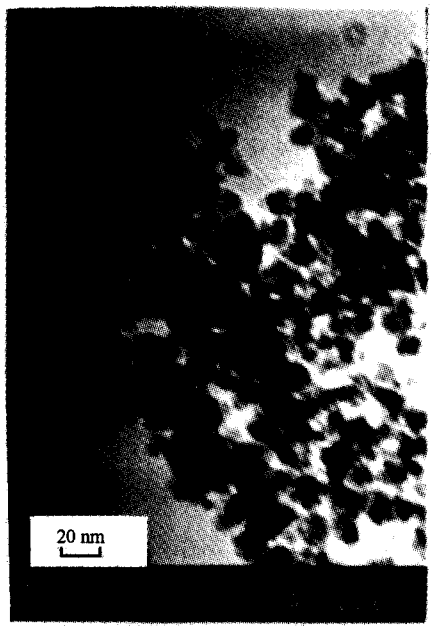

Fig. 2 TEM photo of synthesized Fe_3O_4 particles.

Nano-Fe_3O_4 (100 mg) were dispersed in 10 mL of anhydrous alcohol under sonication for 120 min. A 5 μL aliquot of this dispersion solution was dropped onto the surface of PIGE and dried in the air at room temperature, forming nano-Fe_3O_4 particles modified electrode, labeled as Fe_3O_4/PIGE.

On the surface of the Fe_3O_4/PIGE, 5 μL of HRP solution (10 mg/mL) prepared in KCl-PBS (pH = 6.1), 5 μL of 5.0% (*W*/*W*) BSA and 5 μL of 10% glutaraldehyde were added successively. Then the electrode was allowed to dry naturally at room temperature. During this course, a cross-linked HRP layer was formed on the surface of the Fe_3O_4/PIGE. After rinsed thoroughly with KCl-PBS (pH = 6.1), the final HRP electrode was obtained,

which was labeled as HRP/Fe_3O_4/PIGE. The HRP/Fe_3O_4/PIGE was stored in the pH 6.1 KCl-PBS at 4 ℃ before use.

Results and discussion

Interaction of HRP *and nano-*Fe_3O_4 *particles*

Heme absorption is a very useful conformational probe for the study of heme proteins and positions of the Soret adsorption band provide information about the environment of heme.[22] Film cast from HRP/Fe_3O_4 gave a heme band at 405 nm, which was close to the Soret band at 404 nm for native HRP in buffer (as shown in Fig. 3). This indicated a heme status for the embedded HRP molecules in nano-Fe_3O_4 matrix similar to that in the native protein. FTIR spectroscopy is a more sensitive means to probe into the secondary structure of proteins. Especially the shapes of the amide I and amide II infrared absorbance bands of HRP provide detailed information on the secondary structure of the polypeptide chain.[23] The amide I band (1700—1600 cm^{-1}) could be ascribed to C = O stretching vibrations of peptide linkages in the protein backbone. The amide II band (1600—1500 cm^{-1}) results from a combination of N—H bending and C—N stretching. As shown in Fig. 4, the shape of amide I and II bands of HRP in the Fe_3O_4 nano-particle matrix (1651.8 and 1539.9 cm^{-1}) was nearly the same as those obtained for protein itself (1651.2 and 1538.8 cm^{-1}).

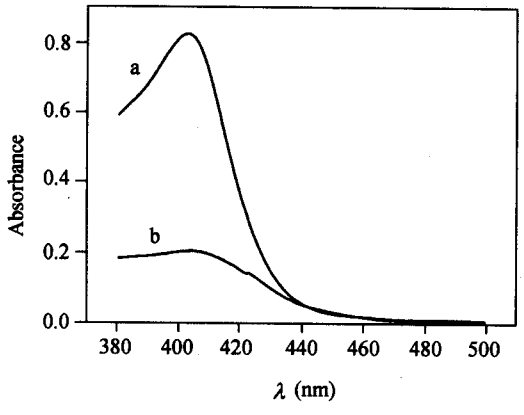

Fig. 3 UV-vis adsorption spectra of HRP in PBS (pH 6.1) (a) and HRP-Fe_3O_4 films (b).

Electrochemical characteristics of HRP/Fe_3O_4/PIGE

The bare PIGE or Fe_3O_4-modified PIGE gave no CV peak. HRP crosslinked with glutaraldehyde alone on PIGE also presented no obvious voltammetric peaks within the potential range studied. Comparatively, the HRP/Fe_3O_4/PIGE gave well-defined redox peaks with E_m, $(E_{pa} + E_{pc})/2$, of − 0.295 V (vs. SCE). This E_m is close to the value obtained by Luo,[14] Rusling *et al*.[24,25] (as shown in Fig. 5). The insert cyclic voltammogram (c) was obtained at scan rate 1.0 V/s by subtracting background CV of Fe_3O_4/PIGE (a) from that of HRP-Fe_3O_4/PIGE (b). Thus, the redox reaction could be inferred as the conversion of the Fe(III)/Fe(II) couple of the heme prosthetic group of HRP. The reduction peak height of the redox process was found to increase linearly over scan rate from 0.5 V/s to 3 V/s (Fig. 6), with a correlation coefficient 0.9960, which was the characteristic of a surface wave. As scan rate is increased, the reduction peak potential shifts negatively. The plot of E_p versus ln (v) (v: scan rate, $V \cdot s^{-1}$) showed a linear regression equation of $E_p/V = -0.378 - 0.0438 \ln[v/(V \cdot s^{-1})]$ with a correlation coefficient, r, of 0.9980.

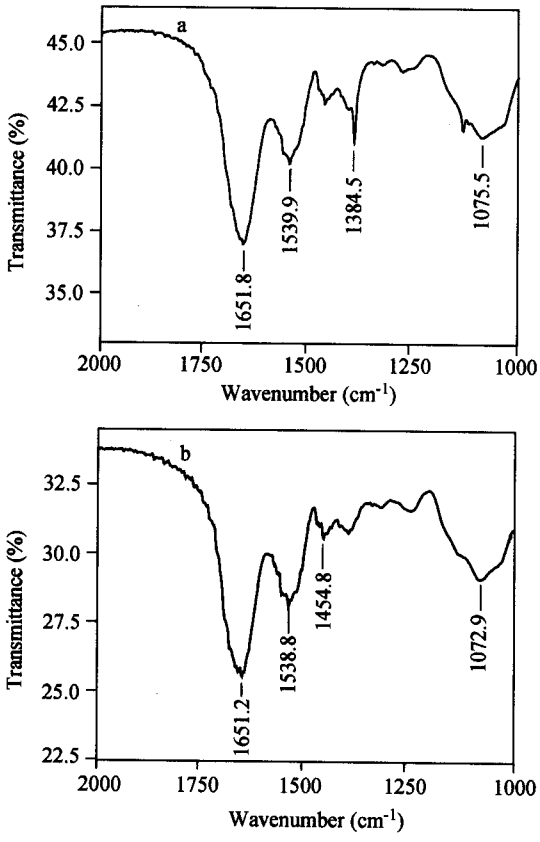

Fig. 4 FTIR spectra of the membranes of HRP-Fe_3O_4 (a) and HRP (b).

In comparison with the equation of $E_p = E^0 + \frac{RT}{\alpha nF} \cdot \ln\frac{RTk_s}{\alpha nF} - \frac{RT}{\alpha nF}\ln \nu$,[26] a value of 0.6 was determined for the charge transfer coefficient, α, for $n = 1$ and $T = 289$ K. Thus the standard electron transfer rate constant, k_s, can be calculated as 2.7 s^{-1}, according to the equation proposed by Laviron:[27]

$$\log k_s^{0'} = \alpha\log(1-\alpha) + (1-\alpha)\log\alpha - \log(RT/nF\nu) - \alpha(-\alpha)nF\Delta E_p/(2.3RT)$$

This value is larger than that of nanocrystalline TiO_2 modified pyrolytic graphite electrode.[14]

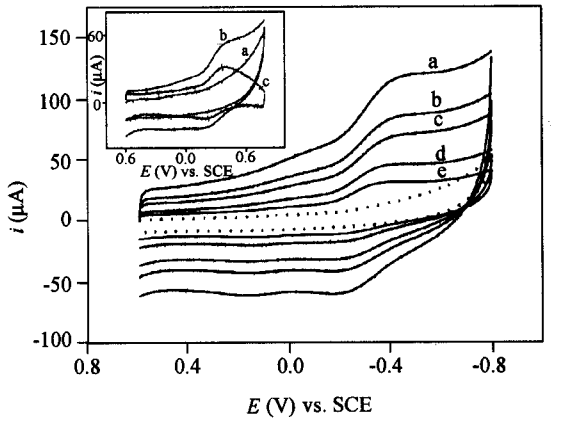

Fig. 5 Cyclic voltammograms of HRP/Fe_3O_4/PIGE at various scan rates: (a), 3; (b), 2; (c), 1.5; (d), 0.8; (e), 0.5 V/s. The dotted line refers to the cyclic voltammogram of the protein-free Fe_3O_4 film modified PIGE at scan rate 0.6 V/s. The insert cyclic voltammograms were obtained at 1.0 V/s at (a), Fe_3O_4/PIGE; (b), HRP/Fe_3O_4/PIGE; (c), substracting the background CV a from b. Solution: pH 6.1, 10 mmol/L PBS containing 50 mmol/L KCl.

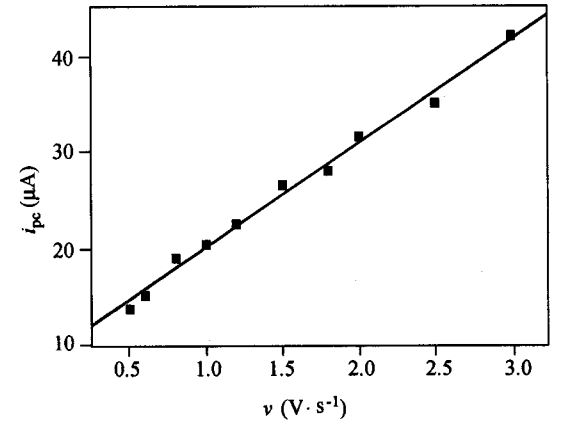

Fig. 6 Plot of cathodic current (i_{pc}) versus scan rate. Experimental conditions: the same as in Fig. 4.

These results provide strong evidence that the capability of electron transfer between HRP and PIGE was enhanced by the existence of nano-Fe_3O_4 matrix. It can be expected that the small size of Fe_3O_4 particles with high surface to volume 0ratio can give the protein molecules more freedom in orientation,[28] which effectively reduces the distance for the ET between HRP and the electrode. On the other hand, HRP has a positive charge at pH 6.1 since its isoelectric point at pH = 7.2, which can be expected to interact with the negatively charged ACP cover layers of the Fe_3O_4 particles. The negatively charged —COO^- groups on the ACP might preferentially absorb HRP cations and become a further driving force for the embedded HRP to assume correct orientation on the surface of the nano-Fe_3O_4 solid matrix. The existence of ACP shell with active —COO^- groups may interact with the amino groups of HRP, which might be favorable chemical bonding interactions to facilitate the electron transfer between entrapped HRP and Fe_3O_4 matrix.

pH *effect*

Direct electrochemistry of the embedded HRP has been well achieved in the pH range of 3.0 to 8.0. Voltammetric peaks for HRP in the nano-Fe_3O_4 matrix shifted negatively with increasing pH value. All changes in voltammetric peak potentials and currents with pH were reversible. For example, CVs for an HRP-Fe_3O_4 film in PBS (pH = 6.1) were reproduced after immersing the film in a PBS (pH = 8.0) and then returning it to the pH 6.1 again. Plots of E_m vs. pH gave a slope of −51.0 mV per pH unit as shown in Fig. 7. This value is close to the theoretical value of −57.6 mV per pH unit at 18 ℃ for a reversible, one-proton-coupled single electron transfer process. It is suggested that one proton transfer is coupled to the electron transfer.

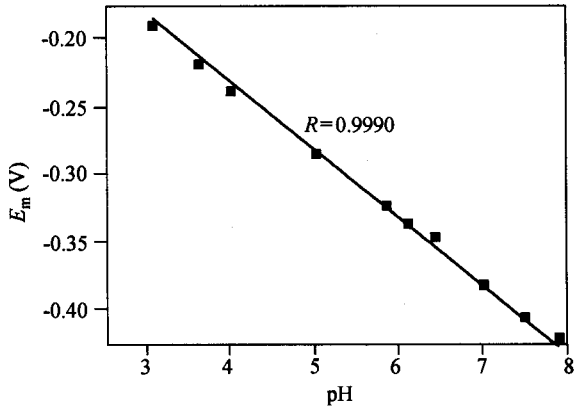

Fig. 7 Plot of med-potential (E_m) versus solution pH.

Electrocatalysis of hydrogen peroxide on HRP/Fe_3O_4/PIGE

Fig. 8 is the CV curves obtained at the HRP/Fe_3O_4/PIGE in PBS (pH = 6.1) 0 with and without H_2O_2. It can be seen that the cathodic peak current at −0.39 V significantly increased after the addition of H_2O_2, showing an electrochemical catalytic wave. Noticeably, no catalytic wave was observed at either a bare PIGE or HRP crosslinked PIGE (free of Fe_3O_4 magnetite). This clearly indicates that the activity of HRP is enhanced by the nano-Fe_3O_4 entrapment. A linear dependence between the catalytic peak current and the concentration of H_2O_2 was observed in the range of 1.0×10^{-5}—1.4×10^{-4} mol/L, as shown in Fig. 8. The linear regression equation is $i/\mu A = 2.78 + 452c/(\text{mmol} \cdot \text{L}^{-1})$ ($r = 0.9990$). Five independent determinations at a H_2O_2 concentration of 3.2×10^{-5} mol/L showed a relative standard deviation of 3.6%, which displays nice reproducibility. The detection limit was 7.3×10^{-6} mol/L of H_2O_2 for signal to noise ratio of

3.

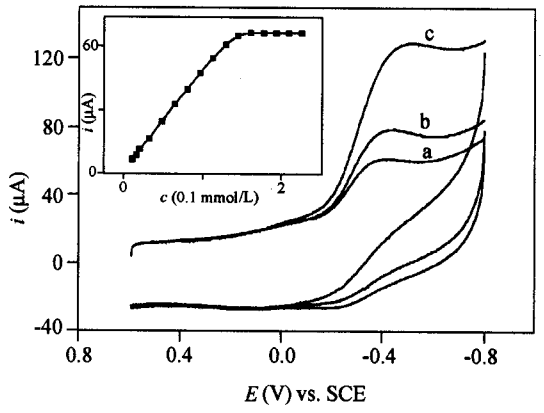

Fig. 8 Cyclic voltammograms of HRP/Fe_3O_4/PIGE in the blanch solution (a) and in the presence of H_2O_2: 0.032 mmol/L (b) and 0.144 mmol/L (c). Solution: PBS (10 mmol/L, pH = 6.1) + KCl (50 mmol/L). Scan rate: 1.0 V/s. Insert is plot: the catalytic peak current versus H_2O_2 concentration.

For evaluation of the biological activity for the immobilized HRP, the apparent Michaelis-Menten constant K_m^{app} can be calculated.[11,29,30]

For the reaction of enzyme (E) and single substrate (S)

$$E + S \underset{k_{-1}}{\overset{k_1}{\rightleftharpoons}} ES \xrightarrow{k_2} E + P$$

It has

$$v = \frac{V_{max}[S]}{[S] + K_m^{app}}$$

or

$$\frac{1}{v} = \frac{1}{V_{max}} + \frac{K_m^{app}}{V_{max}[S]}$$

where v is the reaction rate and at infinite substrate concentration, v reaches its maximum velocity, V_{max}. For electrochemistry, the catalytic currents (i and I_{max}) can be used to evaluate the reaction rate, as expressed by the Lineweaver-Burke equation:[29]

$$\frac{1}{i} = \frac{1}{I_{max}} + \frac{K_m^{app}}{I_{max}[S]}$$

From the plot of $\frac{1}{i}$ versus $\frac{1}{[S]}$, K_m^{app} value can be calculated from the ratio of the slope and intercept of the fitting line.

For our case, a K_m^{app} value of 0.42 mmol/L was calculated for the catalytic oxidation of H_2O_2 at the HRP/Fe_3O_4/PIGE. This value is much smaller than that reported for the system of sol-gel/GCE.[30]

Conclusion

Enhanced electron transfer of HRP and the electrode was achieved at the newly prepared HRP/Fe_3O_4/PIGE. This HRP modified electrode can provide a sensitive and reproducible probing of H_2O_2. It is clear that the presence of nano-Fe_3O_4 facilitates the electron transfer between HRP and PIGE. The HRP immobilization and stabilization is mainly due to the large specific surface area of nano-Fe_3O_4 particles. However, coulombic interactions and chemical bonding effect between the HRP and the nano-Fe_3O_4 matrix should also play an important role. The HRP embedded in the nano-Fe_3O_4 matrix may basically remain its native structure. Thus, it provides a promising way to fabricate enzyme-based biosensors free of mediator. For nano-Fe_3O_4 solid matrix, it is potential in both protein characterization and biosensor applications.

References

1 Ryan, O.; Smyth, M. R.; Fagain, C. D. *Enzyme Microb. Technol* **1994**, *16*, 501.
2 Dunford, H. B. *Peroxidase Chem. Ciol.* **1991**, *2*, 1.
3 Armstrong, F. A.; Hill, H. A. O.; Walton, N. *J. Acc. Chem. Res.* **1998**, *21*, 407.
4 Ruzgas, T. E.; Csoregi, J.; Emneus, L.; Gorton, G. Marko-Varga. *Anal. Chim. Acta* **1996**, *230*, 123.
5 Gleria, K. D. I.; Hill, H. A. O.; Lowe, V. J.; Page, D. J. *J. Electroanal. Chem.* **1986**, *213*, 333.
6 Chen, H.; Ju, H.; Xun, Y. *Anal. Chem.* **1994**, *66*, 4538.
7 Hu, N. F.; Rusling, J. F. *Langmuir* **1997**, *13*, 4119.
8 Ferri, T.; Poscia, A.; Santucci, R. *Bioelectrochem. Bioenerg.* **1998**, *44*, 177.
9 Krishnananda, C.; Shyamalara, M. *Bioelectrochem.* **2001**, *53*, 17.
10 Huang, R.; Hu, N. F. *Bioelectrochem.* **2001**, *54*, 75.
11 Fan, C. H.; Wang, H. Y.; Sun, S.; Zhu, D.; Wagner, X. G.; Li, G. X. *Anal. Chem.* **2001**, *73*, 2850.
12 Yang, J.; Hu, N. F. *Bioelectrochem. Bioenerg.* **1999**, *48*, 117.
13 Wu, Z. Y.; Wang, B.Q.; Cheng, Z. L.; Yang, X. R.; Dong, S. J.; Wang, E. K. *Biosens. Bioelectron.* **2001**, *16*, 47.
14 Li, Q. W.; Luo, G. A.; Feng, J. *Electroanalysis* **2001**, *13*, 359.
15 Roath, S. *J. Magn. Magn. Mater.* **1993**, *122*, 329.
16 Rusetski, A. N.; Ruuge, E. K. *J. Magn. Magn. Mater.* **1990**, *85*, 299.
17 Bilková, Z.; Slováková, M.; Horák, D.; Lenfeld, J.; Churáček, J. *J. Chromatogr., B* **2002**, *770*, 177.
18 Koneracká, M.; Kopčanský, P.; Antalík, M.; Timko, M.; Ramchand, C. N.; Lobo, D.; Mehta, R. V.; Upadhyay, R. V. *J. Magn. Magn. Mater.* **1999**, *201*, 427.
19 Bahar, T.; Celebi, S. S. *Enzyme Microb. Technol.* **1998**,

23, 301.

20 Berger, P.; Adelman, N. B.; Beckman, K. J.; Campbell, D. J.; Ellis, A. B.; Lisensky, G. C. *J. Chem. Educ.* **1999**, *76*, 943.

21 Wang, C. Y.; Zhu, G. M.; Chen, Z. Y.; Lin, Z. G. *Mater. Res. Bull.* **2002**, *37*, 2525.

22 Irace, G.; Bismuto, E.; Sary, F.; Colonna, G. *Arch. Biochem. Biophys.* **1986**, *244*, 459.

23 Kumosinski, T. F.; Unruh, J. J. *Molecular Modeling*, ACS Symp, Washington DC, **1993**, pp. 71—98.

24 Lu, Z.; Huang, Q.; Rusling, J. F. *J. Electroanal. Chem.* **1997**, *423*, 59.

25 Nassar, A.-E. F.; Rusling, J. F. *J. Am. Chem. Soc.* **1996**, *118*, 3043.

26 Dong, S. J.; Che, G.; Xie, Y. *Chemically Modified Electrodes*, Science Press, Beijing, **1995**, p. 129.

27 Laviron, E. *J. Electroanal. Chem.* **1974**, *52*, 355.

28 Koneracká, M.; Kopčanský, P.; Timko, M.; Ramchand, C.N.; Sequeira, A. de; Trevan, M. *J. Mol. Catal. B: Enzym.* **2002**, *18*, 13.

29 CASS, A.E.G. *Biosensors: A Practical Approach*, IRL Press, Oxford, **1990**, p. 218.

30 Li, J.; Tan, S. N.; Ge, H. *Anal. Chim. Acta* **1996**, *335*, 137.

(E0301224 SONG, J. P.; LING, J.)